Acta Medica Okayama

Volume 50, *Issue* 5 1996 *Article* 3

OCTOBER 1996

Rat Parathyroid Gland, with Special Reference to Its Blood Vascular Bed, Pericapillary Space and Intercellular Space

Toshihisa Tanaka* Mari Tsubouchi† Yutaka Tsubouchi‡

Aiji Ohtsuka** Takuro Murakami††

*Okayama University,
†Okayama University,
‡Okayama Univeristy,
**Okayama University,
††Okayama University,

Rat Parathyroid Gland, with Special Reference to Its Blood Vascular Bed, Pericapillary Space and Intercellular Space*

Toshihisa Tanaka, Mari Tsubouchi, Yutaka Tsubouchi, Aiji Ohtsuka, and Takuro Murakami

Abstract

The blood vascular bed, perivascular space and intercellular space of the rat parathyroid gland were studied using scanning electron microscopy of vascular casts, freeze-cracked tissue samples, and NaOH-digested tissue blocks. The findings were supplemented by transmission light and electron microscopy of iron colloid-treated or enzyme-digested tissue sections. The rat parathyroid gland contained a rich network of capillaries. These capillaries were surrounded by marked pericapillary spaces which were demarcated by basal lamina of both capillaries and parenchymal cells. The pericapillary spaces contained numerous collagen fibrils, and issued many crista-like projections which ran deep into the sheets of parenchymal cells. The intercellular spaces of parenchymal cells contained neither basal lamina nor collagen fibrils. The surfaces of the parenchymal cells showed strong negative charging, and maintained the intercellular spaces. The luminal surfaces of the capillary endothelium also showed strong negative charging, and maintained the capillary lumen.

KEYWORDS: parathyroid gland, cationic and anionic iron colloid stainings, vascular casting, freeze fracture, maceration

---

*PMID: 8914677 [PubMed - indexed for MEDLINE]

ACTA MED OKAYAMA 1996; 50(5): 243 253

Rat Parathyroid Gland, with Special Reference to Its Blood Vascular Bed, Pericapillary Space and Intercellular Space

Toshihisa TANAKA*, Mari TSUBOUCHI, Yutaka TSUBOUCHI, Aiji OHTSUKA and Takuro MURAKAMI

Department of Anatomy, Okayama University Medical School, Okayama 700, Japan

The blood vascular bed, perivascular space and intercellular space of the rat parathyroid gland were studied using scanning electron microscopy of vascular casts, freeze-cracked tissue samples, and NaOH-digested tissue blocks. The findings were supplemented by transmission light and electron microscopy of iron colloid-treated or enzyme-digested tissue sections. The rat parathyroid gland contained a rich network of capillaries. These capillaries were surrounded by marked pericapillary spaces which were demarcated by basal lamina of both capillaries and parenchymal cells. The pericapillary spaces contained numerous collagen fibrils, and issued many crista-like projections which ran deep into the sheets of parenchymal cells. The intercellular spaces of parenchymal cells contained neither basal lamina nor collagen fibrils. The surfaces of the parenchymal cells showed strong negative charging, and maintained the intercellular spaces. The luminal surfaces of the capillary endothelium also showed strong negative charging, and maintained the capillary lumen.

Key words: parathyroid gland, cationic and anionic iron colloid stainings, vascular casting, freeze fracture, maceration

The parathyroid gland is rich in capillaries (1–4). They were three-dimensionally visualized utilizing our previous scanning electron microscopy of vascular casts in the rat (5). Our recent scanning electron microscopy of vascular casts combined with light and electron microscopy of tissue sections indicated that the parathyroid capillaries are provided with marked tissue spaces (6). The present study reinvestigates those hitherto poorly understood structures in the rat parathyroid gland by scanning electron microscopy of vascular casts, freeze-cracked tissue samples and NaOH-macerated tissue blocks and by transmission light and electron microscopy of iron colloid-treated or enzyme-digested tissue sections. Some findings of intercellular spaces will also be included.

Materials and Methods

Adult male Wistar rats weighing 250–300 g were used. They were anesthetized with ethyl ether.

Light Microscopy

The anesthetized animals were perfused through the ascending aorta with Ringer's solution and with 2.5% glutaraldehyde or 4% paraformaldehyde in 0.1 M cacodylate buffer (pH 7.2). The parathyroid glands were then isolated together with some thyroid tissue. The isolated glands were immersed for 6 h or longer in the same fixative, dehydrated in paraffin, and cut into 10–15-μm-thick sections. The sections thus prepared were deparaffinized and treated as follows.

Iron colloid stainings. The sections from the glutaraldehyde-fixed specimens were incubated in fine cationic iron colloid with pH values of 1.0–1.5, 4.0–4.5 or 7.2–7.4 (7) or anionic iron colloid with pH values of 7.2–7.4 (8), treated for Prussian blue reaction, and counterstained with nuclear fast red.

Some sections were stained with hematoxylin and eosin.

Methylation and saponification. Some sections from the glutaraldehyde-fixed specimens were methylated with 0.05 N HCl in methanol at 58–60°C (9), and saponified with 0.1 N KOH in 70% ethanol at room temperature (10). In each step, the sections were stained with cationic iron colloid at pH values of 1.0–1.5 or 7.2–7.4 and treated for Prussian blue reaction (7).

* To whom correspondence should be addressed.

Enzyme digestions. The sections from the paraformaldehyde-fixed specimens were digested with sialidase (11) or hyaluronidase (12). The sections were then incubated in cationic iron colloid at pH values of 1.0 -1.5 or 7.2-7.4 and treated for Prussian blue reaction (7).

Transmission Electron Microscopy

The parathyroid glands were isolated, without any perfusion, from anesthetized rats and cut into blocks ($0.3 \times 0.3 \times 0.3$ mm). They were fixed with 2.5 % glutaraldehyde in 0.1 M cacodylate buffer (pH 7.2) at 4 °C for 6 h, postfixed with 1 % osmic acid in the same buffer at 4 °C for 3 h, embedded in epoxy resin and cut into ultrathin sections. These sections were stained with uranyl acetate and lead citrate and observed with a transmission electron microscope (Hitachi, H-700) using an acceleration voltage of 100 kV.

Small blocks were prepared from the Ringer-perfused and glutaraldehyde-fixed parathyroid glands. These blocks were intensely stained with osmic acid or treated with 1 % tannic acid for 6 h and 1 % osmic acid for 3 h (13), embedded in epoxy resin and cut into ultrathin sections for transmission election microscopy without any additional metal coating.

In some cases, the parathyroid glands were isolated after glutaraldehyde-perfusion fixation. These glands were cut into small blocks (see above), refixed with glutaraldehyde, embedded in LR White resin and cut into ultrathin sections. These sections were treated with cationic iron colloid at pH values of 1.0-1.5 or 4.0-4.5, exposed to osmium vapor and observed with the H-700 transmission electron microscope at 100 kV acceleration voltage (14).

Scanning Electron Microscopy

Vascular casts. Some of the anesthetized animals were perfused through the ascending aorta with Ringer's solution after ligation of thoracic aorta. They were then infused with laboratory-prepared low viscosity methacrylate casting medium (15, 16) or commercially available one (Mercox, Oken Shoji) until the superior vena cava was filled with the casting medium. These resin-infused animals were corroded in a NaOH solution, washed in running tap water, and air-dried (15). The blood vascular casts thus prepared were dissected, and the blood vascular beds of the parathyroid glands were isolated together with those of the thyroid glands. The isolated casts were exposed to osmium vapor (16), sputter-coated with gold and observed with a scanning electron microscope at an acceleration voltage of 5 kV.

Freeze-cracked tissue samples. Ringer-perfused and glutaraldehyde-fixed parathyroid glands (see above) were conductively stained with 1 % tannic acid and 1 % osmic acid (18), freeze-fractured in liquid nitrogen (19), critical point-dried, sputter-coated with gold and scanned at an acceleration voltage of 25 kV.

Macerated tissue samples. After immersion fixation with glutaraldehyde (see above), the parathyroid glands were macerated by a modified NaOH cell-digestion method (19). Briefly, the Ringer-perfused and glutaraldehyde-fixed glands were immersed in a 2 N NaOH aqueous solution at 23 °C for 3 days and washed in distilled water at 23 °C for 3 days. They were conductively stained with tannin-osmium (17), freeze-cracked in liquid nitrogen (18), and observed at an acceleration voltage of 25 kV.

Results

Rats possess one pair of parathyroid glands. Each gland is located at the latero-cranial aspect of the thyroid gland.

Light Microscopy

Iron colloid stainings. Light microscopy of hematoxylin/eosin, cationic iron colloid/nuclear fast red or anionic iron colloid/nuclear fast red-stained sections revealed that the rat parathyroid gland is separated from the thyroid gland by a thick connective tissue capsule (Figs. 1, 2). This connective tissue capsule extended into the parathyroid gland and formed septa which conveyed blood vessels and nerves into the parathyroid gland (Figs. 1, 2). The septa contained some mast cells which were both reactive to cationic and anionic iron colloids. Few lymphatic vessels were noted in the gland.

The parenchyma of the parathyroid gland consisted of densely packed secretory (parenchymal) cells forming the sheets (Figs. 1, 2). The cytoplasm of these cells was well reactive to anionic iron colloid with pH values of 7.0-7.4 (Figs. 1, 1 Inset); it was not stained with cationic iron colloid at any pH levels of 1.5-7.4 (Figs. 2, 2 Inset, 3). Thus, no dark cells were identified in the iron colloid stainings and also in the hematoxylin/eosin staining.

Marked intercellular tissue spaces were noted between or among the parenchymal cells, especially in the specimens prepared by perfusion fixation (Figs. 1-3). The surfaces of parenchymal cells (apical and lateral domains) enfacing these intercellular tissue spaces were stained with cationic iron colloid at pH values of 7.2-7.4 (Fig. 2 Inset) and 4.0-4.5; they were not reactive to this colloid at pH

Fig. 1 Light micrograph of parathyroid section from an adult rat, stained with anionic iron colloid with a pH value of 7.2. The parenchyma consists of densely packed parathyroid cells forming the sheets (**P**). Blood capillaries run in the sheets or in close contact with the sheets (arrowheads). Inset shows a pericapillary space (**S**), which contains two capillaries (arrowheads) and a protruding marked crista-like projection (arrow) running into the sheet of parenchymal cells (**P**). **C**, connective tissue surrounding the parathyroid gland; **F**, thyroid follicle; **a**, arterial vessel, **c**, connective tissue septum; **I**, lymphatic vessel; **v**, venous vessel. × 80, Inset: × 200.

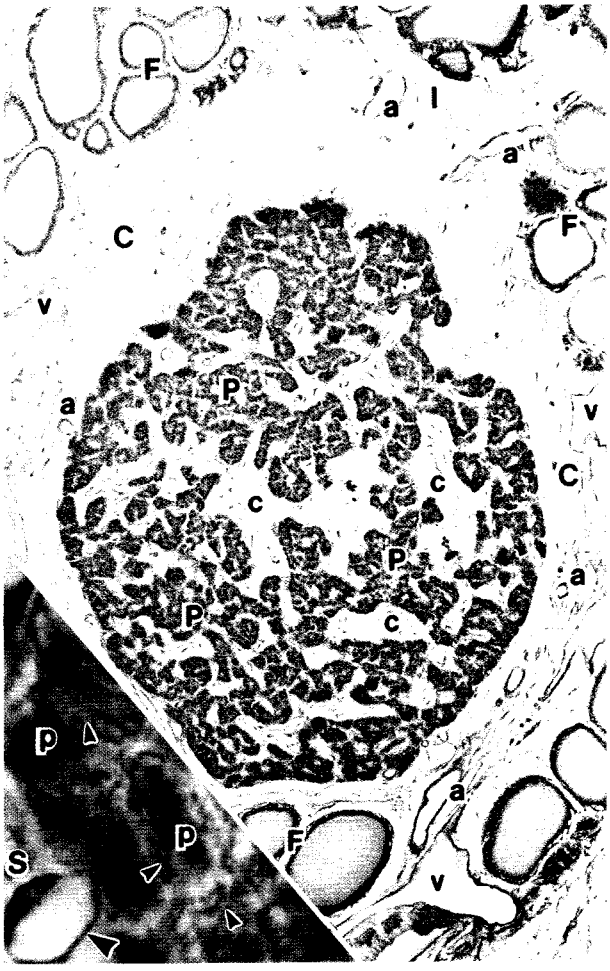

Fig. 2 An adjacent section of Fig. 1, stained with cationic iron colloid with a pH value of 7.2 and counter-stained with nuclear fast red. The parathyroid cells are not reactive to cationic iron colloid. Inset shows a part of this figure. Note in this inset that the surfaces of the parenchymal cells enfacing the intercellular tissue spaces are stained with cationic iron colloid (small arrowheads). The capillary endothelium (large arrowhead) in the pericapillary space (**S**) is also stained with cationic iron colloid. **C**, **F**, **P**, **a**, **c**, **I** and **v** (see the legends for Fig. 1). × 80, Inset: × 300.

values of 1.0–1.5 (Fig. 3). The surfaces of parenchymal cells (basal domains) enfacing the pericapillary spaces (see below) were not reactive to cationic iron colloid at any pH values of 1.0–1.5, 4.0–4.5 and 7.2–7.4.

The parathyroid gland was rich in blood capillaries. The capillaries ran within the sheets of parenchymal cells (Figs. 1–3). These capillaries were bordered by marked pericapillary tissue spaces, which issued some crista-like projections running deep into the parenchymal sheets (Fig. 1 Inset). The luminal surface of these capillaries was reactive to cationic iron colloid at pH values of 1.0–1.5 (Fig. 3) as well as 7.2–7.4 (Fig. 2).

Connective tissue elements or collagen fibrils in the pericapillary tissue spaces were reactive to cationic iron colloid at pH values of 7.2–7.4 (Fig. 2 Inset), but not reactive at pH values of 1.0–1.5 and 4.0–4.5 (Fig. 3).

Collagen fibrils in the septa and other structures, including the parathyroid capsule, were also reactive to cationic iron colloid at pH value of 7.2–7.4.

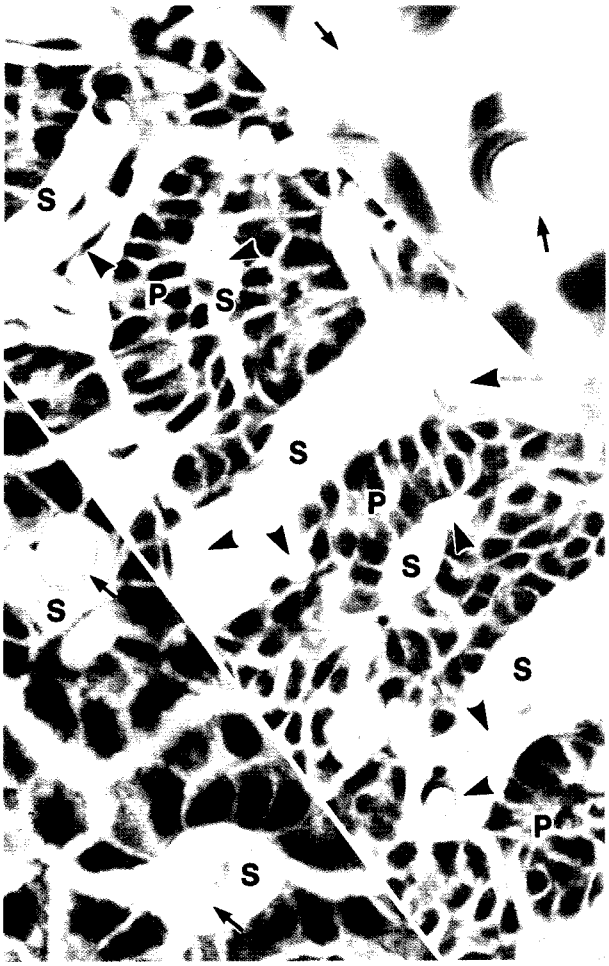

Fig. 3 A section stained with cationic iron colloid with a pH value of 1.5 and counter-stained with nuclear fast red. Pericapillary tissue space (S) contains one or more capillaries (arrowheads). Upper inset is a closer view of a part of this figure, demonstrating that the capillary endothelium is stained with cationic iron colloid even at a pH value of 1.5 (arrows). Lower inset shows a section treated with sialidase and stained with cationic iron colloid at a pH value of 1.5. Sialidase digestion erases the negative charging of capillary endothelium (arrows). P, sheets of parenchymal cells; S, pericapillary spaces. × 200, Upper inset: × 300, Lower inset: × 250.

Methylation, saponification and enzyme digestions. The surface negative charging of the parenchymal cells was eliminated by methylation, and reversed by saponification, whereas it was not eliminated by the hyaluronidase and sialidase digestions.

The negative charging of the luminal surface of the capillary endothelium was eliminated by methylation, and reversed by saponification. This charging was eliminated by sialidase digestion (Fig. 3 Lower inset), and not erased by hyaluronidase digestion.

The negative charging of the collagen fibrils was eliminated by methylation, and reversed by saponification, whereas it was not eliminated by hyaluronidase and sialidase digestions.

Transmission Electron Microscopy

Transmission electron microscopy of non-perfused specimens showed that the capillary endothelium in the parathyroid glands was highly fenestrated, and surrounded by a well defined basal lamina (parenchymal lamina) (Fig. 4). The surfaces of parenchymal cells facing the capillaries were also provided with a well defined basal lamina (endothelial lamina) (Fig. 4). The crista-like projections of the pericapillary spaces were lined by the parenchymal basal lamina (Fig. 4 Inset). Thus, the pericapillary spaces were clearly demarcated by the parenchymal and endothelial basal laminae.

The pericapillary spaces contained many collagen fibrils, some fibroblasts and a few mast cells (Fig. 4 Inset). Few pericytes were identifiable around the capillaries. Unmyelinated nerves or their terminals containing cored or non-cored vesicles were occasionally noted in the pericapillary spaces.

The parenchymal cell surfaces enfacing the intercellular tissue spaces were interdigitated (Fig. 4), and connected to each other by scattered desmosomes (Fig. 4 Inset). The intercellular tissue spaces thus possessed neither basal lamina nor collagen fibrils, or were empty without any tissue elements.

Fig. 4 Transmission electron micrograph of an ultrathin section of the rat parathyroid gland. Crista-like projections protrude into pericapillary tissue space (arrows), and run into the sheets of parenchymal cells (p). Intercellular spaces are occupied with many digitated processes of the parenchymal cells (large arrowheads). Inset shows the right-sided projection (large arrow) as observed in an adjacent section. The parenchymal cells (p) are firmly fixed or connected to each other by desmosomes (small arrow). Double small arrows, endothelial fenestrations; small arrowheads, basement membrane of the parenchymal cells; duplicated small arrowheads, basement membrane of the capillary; F, fibroblastic cells or their processes; f, collagen fibrils. × 15,000, Inset: × 20,000.

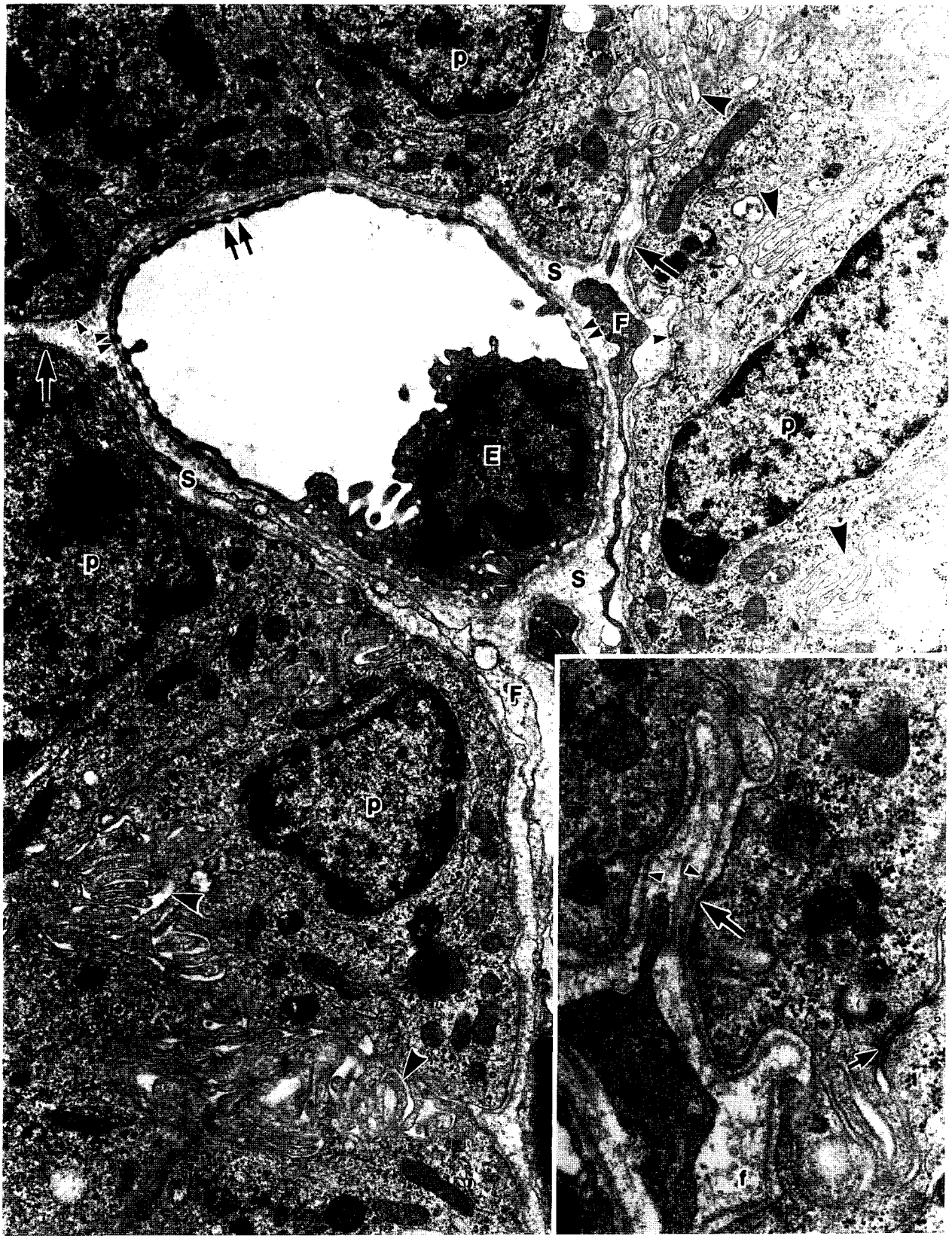
P
S
F
E
P
S
P
S
F
P
f

Fig. 5 Parathyroid gland fixed by arterial perfusion. The perfusion fixation markedly widened the intercellular spaces (**I**). However, desmosomes are well preserved (arrows). Upper inset shows a section embedded in LR White resin, revealing that iron particles (pH 4.5) are additionally deposited on the cell surfaces of parenchymal cells enfacing the intercellular tissue space (arrowheads). Lower inset shows a section obtained from the LR White-embedded specimen and stained with cationic iron colloid with a pH value of 1.5. Iron particles at this pH level are preferentially deposited on the luminal surfaces of the capillary endothelium (arrowheads). **E**, capillary endothelium; **S**, pericapillary space; **p**, parenchymal cell. × 15,000, Upper inset: × 30,000, Lower inset: × 30,000.

Perfusion-fixation caused a marked widening of the intercellular tissue spaces (Fig. 5), leaving desmosomes connecting the cells (Fig. 5 Upper inset).

Transmission electron microscopy of LR White resin-embedded and cationic iron colloid (pH 1.0–1.5)-treated specimens showed that the colloidal particles were preferentially deposited on the luminal surfaces of the capillaries, especially on the proper plasmalemma; few colloidal particles adhered to fenestrae (Fig. 5 Lower inset). In the staining at the pH level of 4.0–4.5, many colloidal parti-

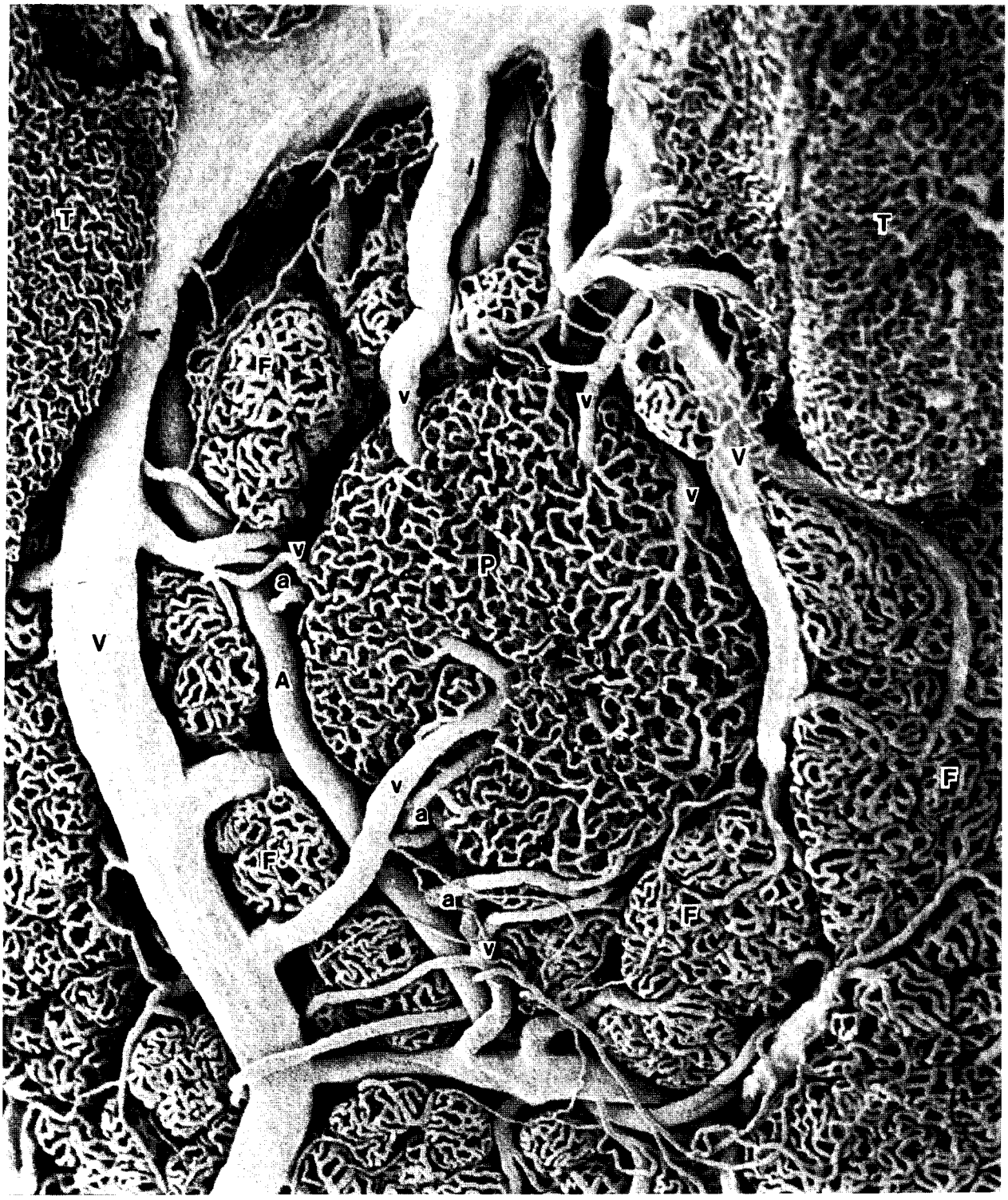

Fig. 6 Scanning electron micrograph of replicated blood vascular bed of the rat parathyroid gland. The parathyroid blood vascular bed (**P**) receives afferent vessels (**a**) from the superior thyroid arteries (**A**) and emits efferent vessels (**v**) draining into the superior thyroid veins (**V**). **F**, capillary networks of thyroid follicles; **T**, capillary beds of fatty tissues. × 120.

Fig. 7 A freeze-fractured tissue block of rat parathyroid gland. The specimen was prepared by perfusion fixation, so that the intercellular spaces were extremely widened (small arrowheads). The pericapillary spaces (**S**) contain one or more capillaries (large arrowheads). Inset shows a closer view of a part of this figure. The pericapillary tissue spaces (**S**) contain many collagen fibrils (**f**). **E**, capillary endothelium; **F**, processes of fibroblasts; **I**, intercellular spaces; **P**, sheet of parenchymal cells; **p**, parenchymal cells; double arrows, endothelial fenestrations. × 600, Inset: × 1,500.

cles were also observed on the surfaces of parathyroid cells (apical and lateral domains) enfacing intercellular tissue spaces (Fig. 5 Upper inset).

Scanning Electron Microscopy

Vascular casts. Sufficient perfusion of low viscosity methacrylate medium through the ascending aorta allowed a good casting of the parathyroid (Fig. 6). Few leakages of the perfused medium were noted.

The capillary bed of each parathyroid gland received four to five afferent vessels from the superior thyroid artery. These afferent vessels branched variously in the superficial and deep layers of the gland and formed a network of freely anastomosing capillaries (Fig. 6). This network converged into venules at various levels in the superficial and deep layers of the gland and finally converged into several emissary veins that were drained, via parathyroid efferent vessels, into the superior thyroid veins (Fig. 6).

The capillary network of the parathyroid gland was independent from that of the thyroid gland. The capillaries in the former gland were thinner than those in the latter. No capillary connection was noted between the capillary plexuses of the parathyroid and thyroid glands.

Freeze-fractured tissues. Freeze-fracture confirmed that the parenchymal cells were arranged in sheets, and that they usually have direct contact with pericapillary spaces (Fig. 7). It also confirmed that the latter spaces contained numerous collagen fibrils (Fig. 7).

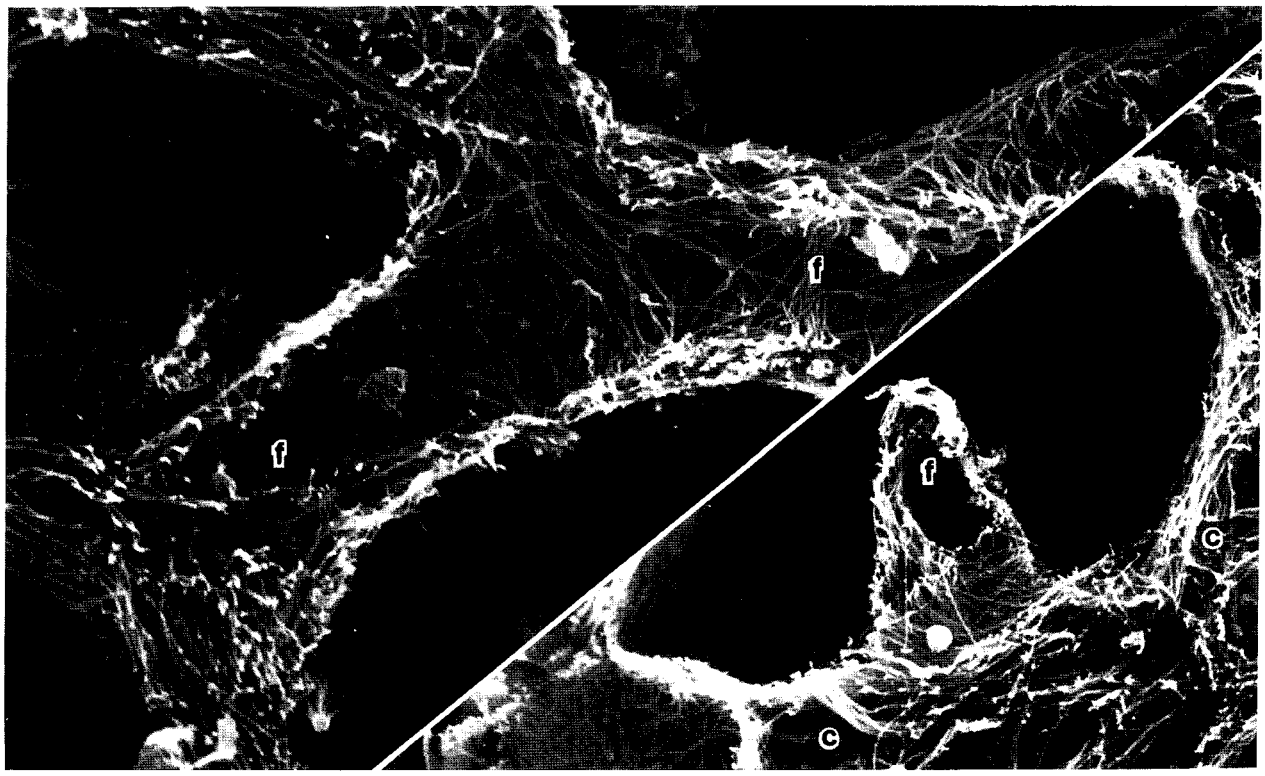

Fig. 8 Pericapillary networks of collagen fibrils (**f**). Inset shows that the collagen networks (**f**) is continuous with the septal collagen networks (**c**). × 5,000, Inset: × 5,000.

Macerated tissues. Digestion with NaOH removed cellular components, leaving only collagen fibrils (Fig. 8). The collagen fibrils thus exposed were 20-100 nm in diameter. The collagen fibrils in the septa were interlaced in a complicated fashion (Fig. 8 Inset). The fibrils in the pericapillary spaces formed a thin network, in which some fibrils ran along the long axis of the capillary, whereas others ran obliquely or circumferentially around the capillary (Fig. 8).

Discussion

The parenchymal cells in the parathyroid gland produce the parathyroid hormone (21, 22). These cells are usually classified at the light microscopic and also electron microscopic levels into dark (principal) and light (oxyphilic) cells (22-28). Moreira *et al.* studied newborn, young, adult and senile rats, and described that the dark cells were more frequently observed as an active form in newborn and young animals, while light ones were more frequently noted as a less active type in the adult and senile animals (29). This view has been widely accepted by many authors (30-31), though some authors contend that such differences in cytoplasmic density are due to the artifacts produced in the process of tissue preparation, especially poor fixation (33).

The present study proves that each parenchymal cell in the rat parathyroid gland is similarly reactive to anionic colloid, indicating that no cell is classified into dark and light cells or into principal and oxyphil cells with respect to charging.

The present study, together with our previous scanning observations of cast samples (5, 6), confirms that the rat parathyroid gland contains a rich capillary network. This finding coincides with those obtained in man, monkey, dog, and other mammals by light microscopy of India ink-injected specimens (1-3).

The present study confirms that the capillary network of the rat parathyroid gland is an independent unit which is isolated from the capillary plexuses of the thyroid follicles. It also indicates that the capillary network of the parathyroid gland consists of freely anastomosing capil-

laries, allowing homogeneous blood flow through the gland. Landau and Morgan noted that human parathyroid capillaries are sinusoidal and as wide as the splenic sinuses (3, 4). In the rat parathyroid, all capillaries are thin. Even in our previous scanning studies of the rat, no sinusoidal capillaries were replicated (5, 6). Isono *et al.* observed the vascular casts with a scanning electron microscope, and described many capillary connections between the parathyroid and thyroid glands of the hamster (34, 35). Such parathyroid-thyroid capillary connections were rare in the rat (5, 6).

The present study reveals that the parenchymal capillaries of the rat parathyroid gland are provided with marked pericapillary tissue spaces-demarcated by basal laminae of capillaries and the parenchymal cells. We consider that these spaces are functional structures homogenously to supply the parenchymal cells. The crista-like projections of the pericapillary spaces may be special structures to nourish the parenchymal cells located far from the capillaries. Krstić observed freeze-fractured rat parathyroid glands with a scanning electron microscope, and reported that the pericapillary spaces were almost free of collagen fibrils (35). However, our present and previous scanning data from the freeze-cracked tissues shows that the pericapillary spaces contain many collagen fibrils (6).

The present study revealed that the arterial perfusion conspicuously widened the intercellular tissue spaces of the parenchymal cells, and that the desmosomes connecting the cells are not detached by this arterial perfusion. This fact proves that the desmosomes are fundamental to maintaining the sheets or continuities of parenchymal cells.

Wild and Schraner cytochemically demonstrated in bovine parathyroid gland that exocytic release of parathyroid hormone takes place at the apicolateral domain of the parenchymal cells, the site of cells opposing blood capillaries (36). Isono *et al.* and Setoguchi *et al.* electron-microscopically showed in the hen and rat parathyroid glands some secretory granules that were in the exocytic passage at the apicolateral surfaces of parenchymal cells (34, 37). Parathyroid hormone thus released may flow into the intercellular tissue spaces and then into pericapillary spaces.

The present study shows that the apicolateral surfaces of the parenchymal cells enfacing the intercellular tissue spaces is negatively charged. This negative charging, probably preventing adhesion of parenchymal cells or maintaining the intercellular space, must derive from some carboxylate groups which are reversed by saponification after methylation, and not digested with hyaluronidase and sialidase. The present study additionally indicates that similar negative-charged carboxylate groups cover the collagen fibrils in the pericapillary spaces, septa and parathyroid capsule.

The present study further shows that the luminal surface, especially its proper plasmalemma, of the capillary endothelium is strongly negative-charged, which is eliminated by sialidase digestion. We believe that this endothelial negative charging prevents adhesion of capillary endothelium and maintains the capillary lumen. It has been widely confirmed in the pancreas, intestinal mucosa, kidney and other organs, including the brain, that the luminal surfaces of the capillaries are coated with either sulfated proteoglycans or sialic acid, and intensely negatively charged (38-42). These anionic cites have been regarded as the charge-barriers for transmural passage of molecular substances through the capillary walls (38-42). We recently showed that the peritoneal cavity is maintained by negatively charged sialomucin on the peritoneal free surface (11).

References

1. Petersen H: Anatomische Studie über die Glandulae parathyroideae. Virchow Arch (1903) **174**, 223 237.
2. Romeis B: Morphologische und experimentelle Studien über die Epithelkörper der Amphibien. I. Die Morphologie der Epithelkörper der Anuren Z Anat (1926) **80**, 547-578.
3. Landau E: Zur Kenntnis der Glandula parathyroidea. Anat Anz (1931) **72**, 424 427.
4. Morgan JRE: The parathyroid glands: I. A study of the normal gland. Arch Pathol (1936) **21**, 10-26.
5. Murakami T, Hinenoya H, Taguchi T, Ohtsuka A and Uno Y: Blood vascular architecture of the rat parathyroid glands: A scanning electron microscopic study of corrosion casts. Arch Histol Jpn (1987) **50**, 495-504.
6. Murakami T, Tanaka T, Taguchi T, Ohtsuka A and Kikuta A: Blood vascular bed and pericapillary space in rat parathyroid glands. Microsc Res Tech (1995) **31**, 112-119.
7. Murakami T, Taguchi T, Ohtsuka A, Sano K, Kaneshige T, Owen RL and Jones AL: A modified method of fine-granular cationic iron colloid preparation: Its use in light and electron microscopic detection of anionic sites in the rat kidney glomerulus and certain other tissues. Arch Histol Jpn (1986) **49**, 13 23.
8. Ohtsuka A and Murakami T: Fine anionic iron colloid and its use in light and electron microscopic detection of cationic sites in the rat kidney. Arch Histol Jpn (1986) **49**, 543-552.
9. Fisher ER and Lillie RD: The effect of methylation on basophilia. J Histochem Cytochem (1954) **2**, 81-87.
10. Spicer SS and Lillie RD: Saponification as means of selectively reversing the methylation blockage of tissue basophilia. J Histochem Cytochem (1959) **7**, 123-125.
11. Ohtsuka A and Murakami T: Anionic sites on the free surface of the

peritoneal mesothelium: Light and electron microscopic detection using cationic colloidal iron. Arch Histol Cytol (1994) **57**, 307-315.
12. Murakami T, Ohtsuka A and Taguchi T: Neurons with intensely negatively charged extracellular matrix in the human visual cortex. Arch Histol Cytol (1994) **57**, 509-522.
13. Murakami T: A metal impregnation method of biological specimens for scanning electron microscopy. Arch Histol Jpn (1973) **35**, 323-326.
14. Ohtsuka A, Kikuta A, Taguchi T and Murakami T: A hydrophilic resin-embedding method of light and electron microscopic detection of tissue anionic sites with cationic colloidal iron: As applied to mouse Paneth cells. Arch Histol Cytol (1993) **56**, 423-430.
15. Murakami T: Application of the scanning electron microscope to the study of the fine distribution of the blood vessels. Arch Histol Jpn (1971) **32**, 445 454.
16. Murakami T, Unehira M, Kawakami H and Kubotsu A: Osmium impregnation of methyl methacrylate vascular casts for scanning electron microscopy. Arch Histol Jpn (1973) **36**, 119 124.
17. Murakami T: A revised tannin-osmium method for non-coated scanning electron microscope specimens. Arch Histol Jpn (1974) **36**, 189 193.
18. Iida N: Freeze-fracture of biological specimens prior to conductive staining. Arch Histol Jpn (1984) **47**, 79 88.
19. Ohtani O: Three-dimensional organization of the connective tissue fibers of the human pancreas: A scanning electron microscopic study of NaOH-treated tissues. Arch Histol Jpn (1987) **50**, 557 566.
20. Turner CD and Bagnara JT: Parathyroid and ultimobranchial glands: PTH, calcitonin, and the cholecalciferols; in General Endocrinology, Turner CD, and Bagnara JT, eds, WB Saunders Co., Philadelphia/ London/ Toronto (1976) pp 225-251.
21. Martin CR: Parathyroid hormone, calcitonin and other regulator of calcium and phosphorus metabolism; in Endocrinology, Martin CR, ed, Oxford University Press, New York/Oxford (1985) pp 463-495.
22. Bargmann W: Die Epithelkörperchen; in Möllendorffs Handbuch der mikroskopischen Anatomie des Menschen, VI/2, Bargmann W, ed, Springer Verlag, Berlin (1939) pp 137 196.
23. Bensley SH: Normal mode of secretion in parathyroid of dog. Anat Rec (1947) **98**, 361-379.
24. Nakagami K: Comparative electron microscopic studies of the parathyroid gland: I. Fine structure of monkey and dog parathyroid glands (Japanese text with English abstract). Arch Histol Jpn (1965) **25**, 435 466.
25. Clark NB and Khairallah LH: Ultrastructure of the parathyroid gland of fresh-water turtles. J Morphol (1972) **138**, 131-140.
26. Narbaitz R: Submicroscopic aspects of chick embryo parathyroid glands. Gen Comp Endocrinol (1972) **19**, 253 258.
27. Roth SI and Schiller AL: Comparative anatomy of the parathyroid glands; in Handbook of Physiology, Sec. 7, Endocrinology, Vol. 7, Aurbach, ed, American Physiology Society, Washington DC. (1976) pp 281-311.
28. Moreira JE and Concalves RP: Ultrastructural changes of the rat parathyroid gland under various fixation methods. Anat Anz (1985) **158**, 413 423.
29. Moreira JE, Concalves RP and Acosta AH: Light- and electron microscopic observations on parathyroid glands in different age groups of rats. Gegenbaurs Morphol Jahrb (1985) **131**, 869-882.
30. Wild P and Manser EM: Ultrastructural morphometry of parathyroid cells in rats of different ages. Cell Tiss Res (1985) **240**, 585 591.
31. Isono H, Shoumura S and Emura S: Ultrastructure of the parathyroid gland. Histol Histopathol (1990) **5**, 95 112.
32. Wild P and Setoguchi T: Mammalian parathyroids: Morphological and functional implications. Microsc Res Tech (1995) **32**, 120 128.
33. Larsson H-O, Lorentzon R and Bonquist L: Structure of the parathyroid glands, as revealed by different methods of fixation: A quantitative light- and electron- microscopic study of untreated Mongolian gerbils. Cell Tiss Res (1984) **235**, 51 58.
34. Shoumura S, Emura S and Isono H: The parathyroid gland under normal and experimental conditions (Japanese text with English abstract). Acta Anat Nippon (1993) **68**, 5 29.
35. Krstić R: Three-dimensional organization of the rat parathyroid glands. Z Mikro Anat Forsch (1980) **94**, 445-450.
36. Wild P and Schraner EM: Parathyroid cell polarity as revealed by cytochemical localization of ATPase, alkaline phosphatase and 5'-nucleotidase. Histochemistry (1990) **94**, 409-414.
37. Setoguti T, Inoue Y and Wild P: The biological significance of storage granules in rat parathyroid cells. Microsc Res Tech (1995) **32**, 148 163.
38. Simionescu N, Simionescu M and Palade GE: Differentiated microdomains on the luminal surface of the capillary endothelium: I. Preferential distribution of anionic sites. J Cell Biol (1981) **90**, 605 613.
39. Simionescu N, Simionescu N, Silbert JE and Palade GE: Differentiated microdomains on the luminal surface of the capillary endothelium: II. Partial characterization of their anionic sites. J Cell Biol (1981) **90**, 614-621.
40. Thurauf N, Dermietzel R and Kalweit P: Surface charges associated with fenestrated brain capillaries: *In vitro* labeling of anionic sites. J Ultrastruct Res (1983) **84**, 103-110.
41. Dermietzel R, Thurauf N and Kalweit P: Surface charges associated with fenestrated brain capillaries: II. *In vivo* studies on the role of molecular charge in endothelial permeability. J Ultrastruct Res (1983) **84**, 111-119.
42. Seno S: Ionized groups on the cell surface: Their cytochemical detection and related cell function. Int Rev Cytol (1987) **100**, 203 248.

Received April 24, 1996; accepted July 16, 1996.